AIMS Materials Science, 3(4): 1587-1614.
DOI: 10.3934/matersci.2016.4.1587
Received: 30 July 2016
Accepted: 07 November 2016
Published: 22 November 2016

http://www.aimspress.com/journal/Materials

Research article

A study on the behavior of laminated and sandwich composite plates using a layerwise theory

M.A.S. Venâncio [1] and M.A.R. Loja [1,2,*]

[1] GI-MOSM, Grupo de Investigação em Modelação e Optimização de Sistemas Multifuncionais, ISEL, IPL, Instituto Superior de Engenharia de Lisboa, Portugal
[2] LAETA, IDMEC, Instituto Superior Técnico, Universidade de Lisboa, Portugal

* **Correspondence:** Email: amelialoja@dem.isel.ipl.pt.

Abstract: The numerical study of structures constituted from composite materials, regardless the underlying shear deformation theory used may be framed into an equivalent single-layer or a layerwise methodology. The adoption of one of these approaches is mainly ruled by the detail one needs to put in the description of the deformation kinematics and on the subsequent description of other relevant quantities such as stresses or frequencies. Being important to address both qualitative and quantitatively the influence of different parameters involved in the models and materials used to represent a structure, it is also relevant to understand how layerwise theories can predict its static and dynamic response. These different issues may be addressed by carrying out parametric studies to characterize the influence of specific parameters on the mechanical performance of sandwich and laminated composite plates. To this purpose a layerwise theory based on the first order shear deformation theory, is considered, and a set of different test cases are analyzed in light of this approach, providing results which may also be useful for later comparison purposes.

Keywords: fibrous composite materials; sandwich plates; laminated composite plates; layerwise theory; finite element method

1. Introduction

Composite laminates and sandwich plates constitute a commonly used structural component with many applications in several areas of engineering. Whether considering one or the other type of plate, we have a multilayer configuration, where it is possible to tailor their constitution in order to

achieve a better performance, fitted to specific operating requirements and to ensure a satisfactory service life. A typical sandwich structure consists of one or more layers of high-strength and high-stiffness face sheets, or skins, bonded to a core which may have significantly different elastic properties. In this layered configuration we may also consider the stacking of differently oriented fiber reinforced materials, as well as a combination of different composite materials. In any case it may be important to achieve a more realistic characterization of these structures response, namely concerning the description of the plate deformation kinematics, and therefore on the corresponding states of strain and stress distributions. The study of layered composite structures continues to attract the attention of many researchers, although the extent of the work developed so far. This may be due to continuous advances in the constitution of new materials and on their physical characterization, to the advances in technological processes, and probably also because the availability of more powerful computational resources, enables the use of more expensive algorithmic procedures and the manipulation of greater data volumes.

In the context of equivalent single-layer approaches focused on the study of sandwich or laminated composite structures, we may find many published works. Within this broad branch, we may find works based on different basis theories ranging from the classical one to the higher order shear deformation theories. Just to name a few of them, we may refer the work carried out by Reissner [1] who studied the effect of the transverse shear deformations in plates consisting of anisotropic laminations symmetrical about their midplane. Closely related to this work, Whitney [2] has developed a bending theory for simply supported laminated plates, which included transverse shear deformations. He obtained closed form solutions for bending deflections, flexural vibration frequencies, and buckling loads. Later, Lo et al. [3] presented a higher order theory devoted to the study of the of laminated plates deformation, comparing the results obtained with elasticity solutions. Pandya and Kant [4] developed a higher order shear deformation model for the analysis of the bending analysis of symmetric sandwich plates. Their model assumed a non-linear variation of the in-plane displacements and a constant transverse one. Also in the context of the equivalent single-layer (ESL) approaches, Bernardo et al. [4,5] presented a study on the linear static and free vibrations behavior of functionally graded plates. To this purpose they have used plate models based on the first order shear deformation theory and implemented via traditional Lagrangean elements, kriging-based elements and via a meshless approach with radial basis functions. Loja et al. [6] analysed the transient dynamic behavior of sandwich structures, having a metallic core and functionally graded outer layers. The properties of the particulate composite metal-ceramic outer layers, were estimated using Mori-Tanaka scheme and the dynamic analyses considered first order and higher order shear deformation theories implemented though kriging finite element method. The transient dynamic response of these structures is carried out through Bossak-Newmark method. A framework for the formulation and the dynamic analysis computations of moderately thick laminated doubly-curved shells and panels was proposed by Viola et al. [7]. To that purpose a higher-order shear deformation theory was considered and the differential geometry was used to define the arbitrary shape of the middle surface of shells and panels with different curvatures. Following this single-layer approach, but in the context of non-linear theories, we can refer the work presented by Reddy [8] which proposed a higher-order shear deformation theory of plates accounting for the von Karman strains. Ferreira and Barbosa [9] presented a finite element model for the geometric non-linear analysis of composite shell structures. The non-linear incremental equilibrium equations were established using a total Lagrangian displacement formulation and the solution was obtained

via the incremental/iterative Newton-Raphson method as well as a spherical formulation of the arc-length methods. Recently, Dehkordi et al. [10] proceeded to a nonlinear dynamic analysis of sandwich plate with flexible core and laminated composite face sheets embedded with shape memory alloy wires. This study was based on the mixed layerwise and equivalent single layer (LW/ESL) models in the framework of Carrera's Unified Formulation. It is also relevant to mention the work developed by Thai and his colleagues [11–15] in the context of the isogeometric analysis of laminated structures. This research field is expanding due to its versatility and integrative character; which goes from the computer aided design to the computer aided engineering wherein one may consider included the analysis of structures.

The importance and adequacy of layerwise approaches to multilayer structural elements, as more efficient alternative methodologies when compared to the equivalent single layer ones, has been an object of study and discussion, and some comprehensive studies and reviews were published upon this subject, namely the ones due to Carrera [16,17]. In the first mentioned work of Carrera, he carried out an historical review on the zig-zag theories developed for the analysis of multilayered structures, wherein they describe a piecewise continuous displacement field in the plate thickness direction and fulfill interlaminar continuity of transverse stresses at each layer interface. In the second one referred in the present study, he made a review on the derivation of governing equations and finite element matrices for some of the most relevant plate/shell theories. He also addressed extensive numerical evaluations of available results, along with assessment and benchmarking. In a comprehensive study, Demasi et al. [18] assessed the accuracy of the variational asymptotic plate and shell analysis, when compared to different higher-order, zig-zag and layerwise theories generated through the invariant axiomatic framework denoted as generalized unified formulation. The axiomatic models were also compared to the elasticity solution developed for the case of sandwich structures with high face to core stiffness ratio. Among other works that have already been carried out within the layerwise theories, in the broad sense, we refer some. Filippi et al. [19] proposed one-dimensional layerwise theories using higher-order zig-zag functions defined over fictitious/mathematical layers of the cross-sectional area of laminated beams. Variable kinematics theories have been obtained using piecewise continuous power series expansions of an arbitrary order. Ferreira [20] combined a layerwise theory with the multiquadrics discretization to analyse laminated composite and sandwich plates. To this aim, he used radial basis functions to approximate the differential governing equations and the boundary conditions. Vuksanović and Ćetković [21] proposed Navier-type closed-form solution for static analysis of simply supported composite plate, based on generalized laminate plate theory. The mathematical model assumed a piecewise linear variation of the in-plane displacement components and a constant transverse displacement through the thickness. Nosier et al. [22] considered Reddy's layer-wise theory to carry out free-vibration analysis of laminated plates, which results were further compared with those obtained from a full-fledged three-dimensional elasticity analysis and various ESL theories. The use of LW approaches to study the dynamic behavior of damped structures has also been used by some researchers, namely by Sainsbury and Zhang [23], Daya and Potier-Ferry [24], Barkanov et al. [25] and Araújo et al. [26]. Sainsbury and Zhang [23] proposed a finite element for damped sandwich beam structures combining polynomial shape functions of conventional finite element analysis with Galerkin orthogonal functions. They accounted for displacement consistency over the interfaces between the damping layer and the elastic layers to guarantee good accuracy. Daya and Pottier-Ferry [24] proposed a numerical method for the exact solution of nonlinear eigenvalue

problems. This method associates homotopy and asymptotic numerical techniques and it was applied to the calculation of the natural frequencies and the loss factors of viscoelastically damped sandwich structures. An inverse technique to characterize the nonlinear mechanical properties of viscoelastic core layers in sandwich panels was developed by Barkanov et al. [25]. This technique was based in vibration tests, allowing preserving the frequency and temperature dependences of the storage and loss moduli of viscoelastic materials. The use of an optimization approach based on the planning of the experiments and the response surface technique to minimize the error functional, enabled additionally the reduction of the computational cost. More recently, Araújo et al. [26] carried out optimization and parameter estimation studies of frequency dependent passive damping of sandwich structures with viscoelastic core. To this purpose he used a mixed-layerwise finite element model and the complex modulus approach to model the viscoelastic material behavior.

In the present work, the authors consider a layerwise theory based on the assumptions of the first order shear deformation theory, layer by layer. The global kinematic through the thickness is therefore approximated in a piecewise manner, being potentially advantageous when compared to other equivalent single-layer higher order theories. A study both on the linear static and free vibrations behavior of three-layered configuration composite plates is presented. The viscoelastic behavior of softer cores is not considered in the present work. A parametric assessment on the influence of different geometrical and material factors is carried out.

2. Materials and Methods

2.1. Composite Materials and Constitutive Relations

A laminated composite can be constructed by superposing layers of materials, which can be for example, orthotropic fibrous composite materials or isotropic materials, among other possibilities. Underlying these layers superposition, it is considered that a set of assumptions is verified, namely, that there exist a perfect adhesion among constituent phases and between adjacent layers, the inexistence of voids, the continuity of displacements and the validity of a linear elastic regime, in the structure operating conditions. In Figure 1, we can observe a typical stacking sequence of laminae, each possessing a different fiber orientation.

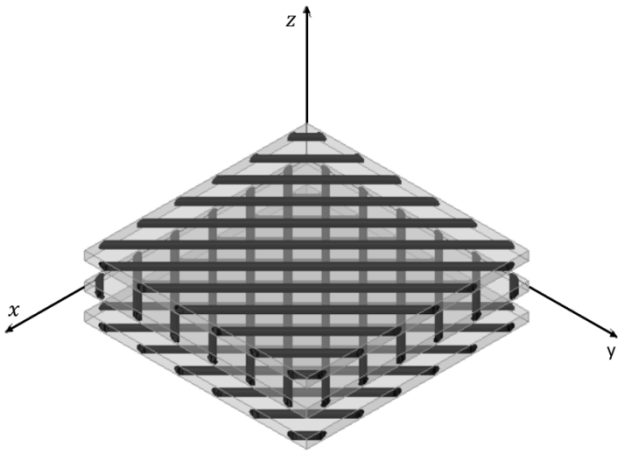

Figure 1. Schematic representation of layers stacking sequence.

In the present study, one considers a layerwise formulation which assumes negligible the transverse normal deformations, within each layer, thus leading to a constant transverse displacement [27,28]. Neglecting as well the transverse normal stress one has for an orthotropic k-th layer, the stress-strain relations in the material coordinate system (1, 2, 3):

$$\begin{Bmatrix} \sigma_1^{(k)} \\ \sigma_2^{(k)} \\ \tau_{12}^{(k)} \\ \tau_{23}^{(k)} \\ \tau_{31}^{(k)} \end{Bmatrix} = \begin{bmatrix} Q_{11} & Q_{12} & 0 & 0 & 0 \\ Q_{12} & Q_{22} & 0 & 0 & 0 \\ 0 & 0 & Q_{66} & 0 & 0 \\ 0 & 0 & 0 & Q_{44} & 0 \\ 0 & 0 & 0 & 0 & Q_{55} \end{bmatrix}^{(k)} \begin{Bmatrix} \varepsilon_1^{(k)} \\ \varepsilon_2^{(k)} \\ \gamma_{12}^{(k)} \\ \gamma_{23}^{(k)} \\ \gamma_{31}^{(k)} \end{Bmatrix} \tag{1}$$

where the subscripts 1 and 2 denote respectively the directions of the fiber and the in-plane normal to fiber, and the subscript 3 is associated to the ply transverse normal direction. $Q_{ij}^{(k)}$, represent the reduced elastic stiffness coefficients of the k-th layer. As each layer may have a different fiber orientation, as we can observe in Figures 1 and 2, it is thus necessary to carry out a transformation procedure so that the necessary analyses involving the whole laminate can be performed.

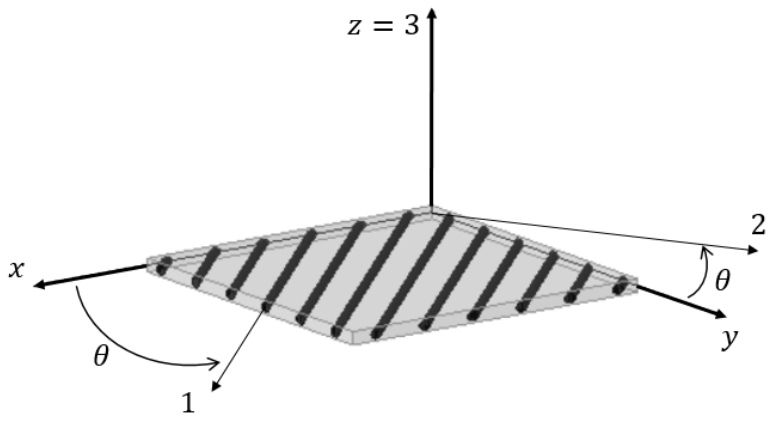

Figure 2. Schematic representation of material and laminate coordinate systems.

The angle θ that characterizes the fiber orientation angle is measured between the positive senses of directions 1 and x. By performing the adequate coordinate transformation the constitutive relations in the laminate xyz coordinate system is finally given as in [29], where $\bar{Q}_{ij}^{(k)}$ represents the transformed reduced elastic stiffness coefficients, associated to each k-th layer.

$$\begin{Bmatrix} \sigma_{xx}^{(k)} \\ \sigma_{yy}^{(k)} \\ \tau_{xy}^{(k)} \\ \tau_{yz}^{(k)} \\ \tau_{zx}^{(k)} \end{Bmatrix} = \begin{bmatrix} \bar{Q}_{11}^{(k)} & \bar{Q}_{12}^{(k)} & \bar{Q}_{16}^{(k)} & 0 & 0 \\ \bar{Q}_{12}^{(k)} & \bar{Q}_{22}^{(k)} & \bar{Q}_{26}^{(k)} & 0 & 0 \\ \bar{Q}_{16}^{(k)} & \bar{Q}_{26}^{(k)} & \bar{Q}_{66}^{(k)} & 0 & 0 \\ 0 & 0 & 0 & \bar{Q}_{44}^{(k)} & \bar{Q}_{45}^{(k)} \\ 0 & 0 & 0 & \bar{Q}_{45}^{(k)} & \bar{Q}_{55}^{(k)} \end{bmatrix}^{(k)} \begin{Bmatrix} \varepsilon_{xx}^{(k)} \\ \varepsilon_{yy}^{(k)} \\ \gamma_{xy}^{(k)} \\ \gamma_{yz}^{(k)} \\ \gamma_{zx}^{(k)} \end{Bmatrix} \tag{2}$$

The mentioned transformation is carried out layer by layer, being not needed if for example, a specific layer has coinciding axes 1 − x (positive senses) or if one uses a material that can be

considered to be isotropic. Usually, when considering an ESL approach and using a first order shear deformation theory, one uses shear correction factors to overcome the through-thickness constant prediction of the transverse shear stresses and thus to approximate the model response to the 3D elasticity distributions. The present LW model considers the FSDT assumptions within each layer, yielding to a kinematics description wherein the rotations at each layer, are independent. Under these conditions, and according to some research works [25–28], the use of the shear correction factors is not considered. However to enable a comparative study, in the present study one has considered in some cases both approaches, i.e., the use of a shear correction factor equal to 1 and equal to a commonly used value, 5/6.

2.2. Layerwise Theory and Equilibrium Equations

In the present study we have considered that the deformation kinematics of the layered plate would be described through a layerwise approach wherein each of the layers response is based on the first-order shear deformation theory assumptions and by imposing the continuity of displacements at the layer's interfaces. It is relevant to note that the stresses that result from the constitutive relation (Eqn. 2) may not satisfy the continuity of tractions across these interfaces. However the deviations introduced by this approximation is considered acceptable, as reported by other researchers [27,28]. Similar approaches have been used in the context of the dynamic analysis of viscoelastic sandwich beams and plates, by Barkanov et al. [25] and Araújo et al. [26]. The prediction of the transverse shear stresses within each layer yields a constant value, according to the constitutive relation, thus leading to a stepwise distribution profile. However, a continuous distribution may be obtained if one uses the elasticity equilibrium equations in a post-processing phase. To illustrate the specific case of a three-layered configuration, independently of the nature of the constituent materials, we present in Figure 3, a schematic representation of the kinematics of the present approach.

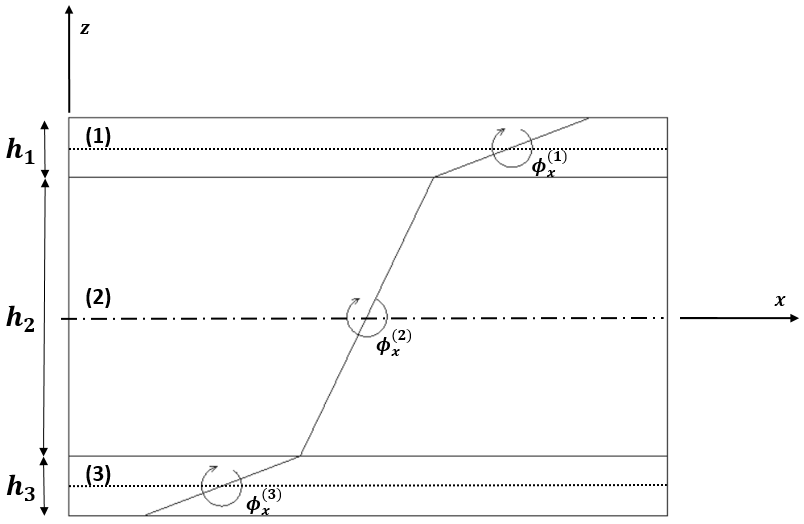

Figure 3. Schematic representation of the deformation kinematics.

The major reason for the use of the first order shear deformation theory is related to its minor computational cost when compared to other approaches. If one considers higher order displacement

fields in layerwise or equivalent single layer theories, the dimension of the problem can become significantly higher. If one would aim to proceed with a failure analysis, for instances, it would be at any time possible, in a post-processing stage, to calculate the transverse normal and shear stresses via the equilibrium equations. Considering this three-layered configuration, and according to the referred kinematics assumptions, the middle layer (core) displacement components, $u^{(2)}$, $v^{(2)}$, $w^{(2)}$, respectively along the x, y, z directions, are described as:

$$\begin{aligned} u^{(2)}(x,y,z,t) &= u_0(x,y,t) + z^{(2)}\theta_x^{(2)}(x,y,t) \\ v^{(2)}(x,y,z,t) &= v_0(x,y,t) + z^{(2)}\theta_y^{(2)}(x,y,t) \\ w^{(2)}(x,y,z,t) &= w_0(x,y,t) \end{aligned} \tag{3}$$

where u and v are the in-plane displacements at any point characterized by the coordinates (x,y,z,t) at a generic time instant t; u_0 and v_0 denote the in-plane displacements of a point in the plate mid-plane $(x,y,0,t)$; w is the transverse deflection; and $\theta_x^{(2)}$ and $\theta_y^{(2)}$ are the rotations of the normals to the core layer mid-plane about the y and x axes, respectively. After the imposition of displacements' continuity at the layers' interfaces, the displacement fields for the upper (1) and lower (3) layers, are respectively given as:

$$\begin{aligned} u^{(1)}(x,y,z,t) &= u_0(x,y,t) + \frac{h_2}{2}\theta_x^{(2)}(x,y,t) + \frac{h_1}{2}\theta_x^{(1)}(x,y,t) + z^{(1)}\theta_x^{(1)}(x,y,t) \\ v^{(1)}(x,y,z,t) &= v_0(x,y,t) + \frac{h_2}{2}\theta_y^{(2)}(x,y,t) + \frac{h_1}{2}\theta_y^{(1)}(x,y,t) + z^{(1)}\theta_y^{(1)}(x,y,t) \\ w^{(1)}(x,y,z,t) &= w_0(x,y,t) \end{aligned} \tag{4}$$

$$\begin{aligned} u^{(3)}(x,y,z,t) &= u_0(x,y,t) - \frac{h_2}{2}\theta_x^{(2)}(x,y,t) - \frac{h_3}{2}\theta_x^{(3)}(x,y,t) + z^{(3)}\theta_x^{(3)}(x,y,t) \\ v^{(3)}(x,y,z,t) &= v_0(x,y,t) - \frac{h_2}{2}\theta_y^{(2)}(x,y,t) - \frac{h_3}{2}\theta_y^{(3)}(x,y,t) + z^{(3)}\theta_y^{(3)}(x,y,t) \\ w^{(3)}(x,y,z,t) &= w_0(x,y,t) \end{aligned} \tag{5}$$

where h_k is the kth-layer thickness and $z^{(k)} \in [-h_k/2, h_k/2]$ are the kth-layer z coordinates. Considering the kinematical relations from the elasticity for small deformations, we obtain for a generic kth layer (omitting time and spatial coordinates' dependency):

$$\begin{Bmatrix} \epsilon_{xx}^{(k)} \\ \epsilon_{yy}^{(k)} \\ \gamma_{xy}^{(k)} \end{Bmatrix} = \begin{Bmatrix} \dfrac{\partial u^{(k)}}{\partial x} \\ \dfrac{\partial v^{(k)}}{\partial y} \\ \dfrac{\partial u^{(k)}}{\partial y} + \dfrac{\partial v^{(k)}}{\partial x} \end{Bmatrix} = \begin{Bmatrix} \epsilon_{xx}^{m(k)} \\ \epsilon_{yy}^{m(k)} \\ \gamma_{xy}^{m(k)} \end{Bmatrix} + z^{(k)} \begin{Bmatrix} \epsilon_{xx}^{b(k)} \\ \epsilon_{yy}^{b(k)} \\ \gamma_{xy}^{b(k)} \end{Bmatrix} + \begin{Bmatrix} \epsilon_{xx}^{mb(k)} \\ \epsilon_{yy}^{mb(k)} \\ \gamma_{xy}^{mb(k)} \end{Bmatrix} \tag{6}$$

$$\begin{Bmatrix}\gamma_{xz}^{(k)}\\ \gamma_{yz}^{(k)}\end{Bmatrix}=\begin{Bmatrix}\dfrac{\partial u^{(k)}}{\partial z}+\dfrac{\partial w^{(k)}}{\partial x}\\ \dfrac{\partial v^{(k)}}{\partial z}+\dfrac{\partial w^{(k)}}{\partial y}\end{Bmatrix}=\begin{Bmatrix}\dfrac{\partial w_0}{\partial x}+\theta_x^{(k)}\\ \dfrac{\partial w_0}{\partial y}+\theta_y^{(k)}\end{Bmatrix}$$

The bending (superscript b) and the membrane (superscript m) components are expressed as:

$$\begin{Bmatrix}\epsilon_{xx}^{b(k)}\\ \epsilon_{yy}^{b(k)}\\ \gamma_{xy}^{b(k)}\end{Bmatrix}=\begin{Bmatrix}\dfrac{\partial\theta_x^{(k)}}{\partial x}\\ \dfrac{\partial\theta_y^{(k)}}{\partial y}\\ \dfrac{\partial\theta_x^{(k)}}{\partial y}+\dfrac{\partial\theta_y^{(k)}}{\partial x}\end{Bmatrix}\quad;\quad\begin{Bmatrix}\epsilon_{xx}^{m(k)}\\ \epsilon_{yy}^{m(k)}\\ \gamma_{xy}^{m(k)}\end{Bmatrix}=\begin{Bmatrix}\dfrac{\partial u_0}{\partial x}\\ \dfrac{\partial v_0}{\partial y}\\ \dfrac{\partial u_0}{\partial y}+\dfrac{\partial v_0}{\partial x}\end{Bmatrix}\tag{7}$$

and the membrane-bending (superscript *mb*) components for outer layers are respectively given by:

$$\begin{Bmatrix}\epsilon_{xx}^{mb(3)}\\ \epsilon_{yy}^{mb(3)}\\ \gamma_{xy}^{mb(3)}\end{Bmatrix}=\begin{Bmatrix}-\dfrac{h_2}{2}\dfrac{\partial\theta_x^{(2)}}{\partial x}-\dfrac{h_3}{2}\dfrac{\partial\theta_x^{(3)}}{\partial x}\\ -\dfrac{h_2}{2}\dfrac{\partial\theta_y^{(2)}}{\partial y}-\dfrac{h_3}{2}\dfrac{\partial\theta_y^{(3)}}{\partial y}\\ -\dfrac{h_2}{2}\left(\dfrac{\partial\theta_x^{(2)}}{\partial y}+\dfrac{\partial\theta_y^{(2)}}{\partial x}\right)-\dfrac{h_3}{2}\left(\dfrac{\partial\theta_x^{(3)}}{\partial y}+\dfrac{\partial\theta_y^{(3)}}{\partial x}\right)\end{Bmatrix}\tag{8}$$

$$\begin{Bmatrix}\epsilon_{xx}^{mb(1)}\\ \epsilon_{yy}^{mb(1)}\\ \gamma_{xy}^{mb(1)}\end{Bmatrix}=\begin{Bmatrix}\dfrac{h_2}{2}\dfrac{\partial\theta_x^{(2)}}{\partial x}+\dfrac{h_1}{2}\dfrac{\partial\theta_x^{(1)}}{\partial x}\\ \dfrac{h_2}{2}\dfrac{\partial\theta_y^{(2)}}{\partial y}+\dfrac{h_1}{2}\dfrac{\partial\theta_y^{(1)}}{\partial y}\\ \dfrac{h_2}{2}\left(\dfrac{\partial\theta_x^{(2)}}{\partial y}+\dfrac{\partial\theta_y^{(2)}}{\partial x}\right)+\dfrac{h_1}{2}\left(\dfrac{\partial\theta_x^{(1)}}{\partial y}+\dfrac{\partial\theta_y^{(1)}}{\partial x}\right)\end{Bmatrix}\tag{9}$$

The equilibrium equations that will enable to perform the static and free vibrations of the laminated or sandwich composite plate, can be obtained through Hamilton principle [29] which can be written as:

$$\int_{t0}^{t1}(\delta U-\delta V+\delta W)dt=0\tag{10}$$

where U,V,W represent respectively the elastic strain energy, the kinetic energy and the work done by external forces applied to the system. Each of these parameters is generically given by:

$$\delta U=\int_\Omega(\delta\boldsymbol{\epsilon}^T\boldsymbol{\sigma})d\Omega\quad;\quad\delta V=\int_\Omega(\rho\delta\dot{\boldsymbol{q}}^T\dot{\boldsymbol{q}})d\Omega\quad;\quad\delta W=\int_A(\boldsymbol{p}\delta\boldsymbol{q})dA\tag{11}$$

with Ω,A being the volume of the plate and the loading application area; ϵ,σ are the generalized strains and stresses' vectors. The density and the pressure loading are respectively represented by ρ

and p. After the constitution of the element matrices and vectors, and their subsequent assembly considering the discretized domain, we can write the equilibrium equation:

$$\boldsymbol{Kq} + \boldsymbol{M\ddot{q}} = \boldsymbol{F} \tag{12}$$

where $\boldsymbol{K}$, $\boldsymbol{M}$, $\boldsymbol{F}$ represent respectively the global elastic stiffness and mass matrices and the global load vector, and $\boldsymbol{q}$, $\boldsymbol{\ddot{q}}$ stand for the generalized displacements and accelerations vectors. The vector of the generalized degrees of freedom is then given as:

$$q^T = [u_0,\ v_0,\ w_0,\ \theta_{x1},\ \theta_{y1},\ \theta_{x2},\ \theta_{y2},\ \theta_{x3},\ \theta_{y3}] \tag{13}$$

Assuming free harmonic vibrations we'll have:

$$\left(\boldsymbol{K} - \omega_i^2 \boldsymbol{M}\right)\boldsymbol{q_i} = 0 \tag{14}$$

with ω_i representing the ith natural frequency associated to the ith vibration mode q_i. For a linear static problem, the equilibrium equation becomes reduced to:

$$\boldsymbol{Kq} = \boldsymbol{F} \tag{15}$$

In any case, these equilibrium equations are solved only after the imposition of the boundary conditions associated to the problem under study.

3. Results and Discussion

The laminated plates considered in the studies carried out possess a three-layered configuration and comprise two main types of plates: a first one where the outer layers are made of orthotropic composite layers and the core is an isotropic foam. In the second group of plates, all the layers are from orthotropic composite materials. The composite layers consider a 60% volume fraction of long reinforcement fibers (carbon or glass) embedded in an epoxy resin. Tables 1 and 2, present the properties used in the present study.

Table 1. Material properties of composites.

Vf = 60%	E_1 (GPa)	E_2 (GPa)	G_{12} (GPa)	υ_{12}	ρ (kg/m^3)
Glass-Epoxy	45.0	12.0	4.5	0.3	2080
Carbon-Epoxy	134.0	7.0	4.2	0.25	1530

Table 2. Material properties of foams.

	H35	H45	H60	H80	H100	H130	H160	H200	H250
Young's modulus (MPa)	49	55	75	95	130	175	205	250	320
Poisson's ratio	0.4	0.4	0.4	0.4	0.4	0.4	0.4	0.4	0.4
Density (kg/m^3)	38	48	60	80	100	130	160	200	250

Concerning to the materials presented in Table 2, which properties were consulted in the manufacturer site [30] and more specifically to the softness of the core, it is important to say that to obtain a more effective prediction of the response of a soft core sandwich it would be advisable to adopt a more adequate approach that takes into account its viscoelastic behavior. The study of soft

core sandwich structures constitutes an investigation field where others researchers have been carrying out different studies. Among others we may refer Daya and Pottier-Ferry [24], Barkanov et al. [24] and Araújo et al. [26]. Considering however just the elastic behavior, a higher order methodology may be an approach to consider in particular if the aspect ratio of the plates is not high. The transverse displacement and the stress components determined in the different case studies, as well as the natural frequencies, are presented in a non-dimensional form using the following multipliers:

$$\bar{w} = \frac{w\left(\frac{l}{2},\frac{l}{2},0\right)}{q},\ \bar{\sigma}_x^1 = \frac{\sigma_x^{(1)}\left(\frac{l}{2},\frac{l}{2},\frac{h}{2}\right)}{q},\ \bar{\sigma}_x^2 = \frac{\sigma_x^{(1)}\left(\frac{l}{2},\frac{l}{2},\frac{h_{core}}{2}\right)}{q},\ \bar{\sigma}_x^3 = \frac{\sigma_x^{(2)}\left(\frac{l}{2},\frac{l}{2},\frac{h_{core}}{2}\right)}{q},$$

$$\bar{\sigma}_y^1 = \frac{\sigma_y^{(1)}\left(\frac{l}{2},\frac{l}{2},\frac{h}{2}\right)}{q},\ \bar{\sigma}_y^2 = \frac{\sigma_y^{(1)}\left(\frac{l}{2},\frac{l}{2},\frac{h_{core}}{2}\right)}{q},\ \bar{\sigma}_y^3 = \frac{\sigma_y^{(1)}\left(\frac{l}{2},\frac{l}{2},\frac{h_{core}}{2}\right)}{q}, \tag{16}$$

$$\bar{\tau}_{xz}^1 = \frac{\tau_{xz}^{(2)}\left(0,\frac{l}{2},0\right)}{q},\ \bar{\tau}_{xz}^2 = \frac{\tau_{xz}^{(2)}\left(0,\frac{l}{2},\frac{h_{core}}{2}\right)}{q},\ \bar{\omega} = \omega h\sqrt{\frac{\rho}{E_2}}$$

The points where these quantities are assessed, as well as its plate spatial correspondence can be respectively exemplified in Figure 4. In Table 3, the presented coordinates are exemplified for a situation where all the layers have equal thickness.

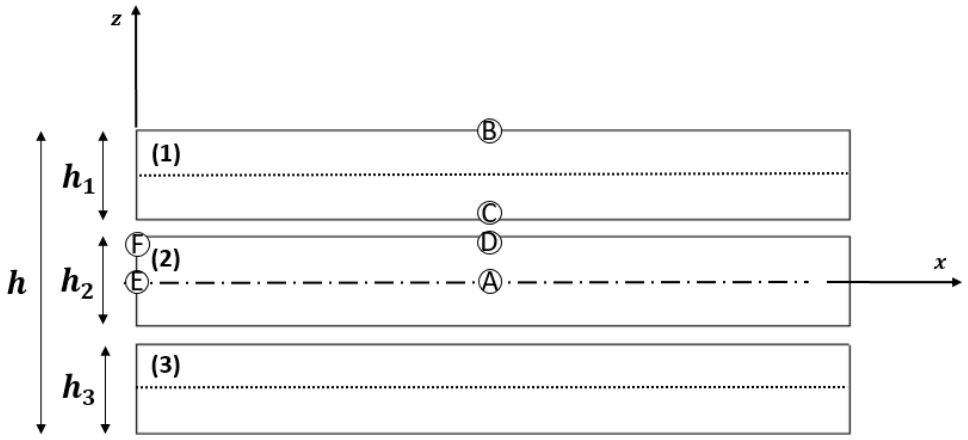

Figure 4. Schematic representation of evaluation points, through plate thickness (h).

Table 3. Points of deflection and stresses evaluation (illustrated xz plane).

A	B	C	D	E	F
$w\left(\frac{l}{2},\frac{l}{2},0\right)$	$\sigma_x^{(1)}\left(\frac{l}{2},\frac{l}{2},\frac{h}{2}\right)$ $\sigma_y^{(1)}\left(\frac{l}{2},\frac{l}{2},\frac{h}{2}\right)$	$\sigma_x^{(1)}\left(\frac{l}{2},\frac{l}{2},\frac{h_{core}}{2}\right)$ $\sigma_y^{(1)}\left(\frac{l}{2},\frac{l}{2},\frac{h_{core}}{2}\right)$	$\sigma_x^{(2)}\left(\frac{l}{2},\frac{l}{2},\frac{h_{core}}{2}\right)$ $\sigma_y^{(1)}\left(\frac{l}{2},\frac{l}{2},\frac{h_{core}}{2}\right)$	$\tau_{xz}^{(2)}\left(0,\frac{l}{2},0\right)$	$\tau_{xz}^{(2)}\left(0,\frac{l}{2},\frac{h_{core}}{2}\right)$

The present layerwise model was implemented using a Lagrange quadrilateral plate finite element model with nine nodes, each having nine degrees of freedom, according to equation 13. The discretization used comprised a 12×12 plate elements mesh, unless otherwise stated. In this work, one considers aspect ratios ranging from five to twenty. As it would be possible to observe, the results obtained, allow to conclude that thicker composites can still be analyzed using this theory. If one considers thinner laminates, a simpler theory may be more adequate.

3.1. Validation Studies

Two first case studies were considered in the present work, to validate the results obtained using the layerwise model taking as reference the results obtained by other authors. The first case is devoted to the static analysis of a sandwich plate, and the second case is focused on the characterization of the eight first natural frequencies of a laminated composite. The discretization considered for the studies carried out was a 12×12 mesh.

3.1.1. Sandwich Plate Under Uniform Load

In this first case, one considered the static analysis of a simply supported square sandwich plate having skin thicknesses of 0.1 h each, and a core thickness equal to 0.8 h, being (h) the total thickness. The plate is submitted to a uniformly distributed transverse load. The elastic stiffness coefficients of the sandwich core are expressed in the matrix, $\bar{Q}_{core}$, as [31]:

$$\bar{Q}_{core} = \begin{bmatrix} 0.999781 & 0.231192 & 0 & 0 & 0 \\ 0.231192 & 0.524886 & 0 & 0 & 0 \\ 0 & 0 & 0.62931 & 0 & 0 \\ 0 & 0 & 0 & 0.266810 & 0 \\ 0 & 0 & 0 & 0 & 0.159914 \end{bmatrix}$$

The skins' elastic stiffness coefficients are related to the core coefficients by a factor R as follows:

$$\bar{Q}_{skin} = R\bar{Q}_{core}$$

The results obtained, namely the transverse displacements and the stresses are presented in a non-dimensional form using the multipliers,

$$\bar{w} = w\left(\frac{l}{2}, \frac{l}{2}, 0\right)\frac{0.999781}{hq},$$

$$\bar{\sigma}_x^1 = \frac{\sigma_x^{(1)}\left(\frac{l}{2}, \frac{l}{2}, \frac{h}{2}\right)}{q},\ \bar{\sigma}_x^2 = \frac{\sigma_x^{(1)}\left(\frac{l}{2}, \frac{l}{2}, \frac{4h}{10}\right)}{q},\ \bar{\sigma}_x^3 = \frac{\sigma_x^{(2)}\left(\frac{l}{2}, \frac{l}{2}, \frac{4h}{10}\right)}{q},\ \bar{\sigma}_y^1 = \frac{\sigma_y^{(1)}\left(\frac{l}{2}, \frac{l}{2}, \frac{h}{2}\right)}{q},$$

$$\bar{\sigma}_y^2 = \frac{\sigma_y^{(1)}\left(\frac{l}{2}, \frac{l}{2}, \frac{4h}{10}\right)}{q},\ \bar{\sigma}_y^3 = \frac{\sigma_y^{(2)}\left(\frac{l}{2}, \frac{l}{2}, \frac{4h}{10}\right)}{q},\ \bar{\tau}_{xz}^1 = \frac{\tau_{xz}^{(2)}\left(0, \frac{l}{2}, 0\right)}{q},\ \bar{\tau}_{xz}^2 = \frac{\tau_{xz}^{(2)}\left(0, \frac{l}{2}, \frac{4h}{10}\right)}{q}$$

In Tables 4–6 one summarizes the transverse displacements and the stresses in non-dimensional form, for different ratios (R) between the elastic stiffness coefficients of the skins and the ones of the

core. The present results are denoted in Tables 4–7 by Q4 and Q9 to denote the two quadrilateral bilinear and biquadratic finite elements used.

As it is possible to conclude, the present results show a general good agreement with the reference solutions. The results obtained with the LW-Q9 model are in good agreement with the ones obtained by Ferreira et al. [27] which used a LW theory and radial basis functions discretization. Although in the present work, one only presents results obtained with nine-node elements, the results obtained with the four-node element implement can be observed also in these tables. A good agreement is found with Ferreira [32] solution which used a bilinear quadrilateral finite element based on a simplified formulation where the membrane degrees of freedom were neglected. Considering a shear correction factor of 5/6, the results will be the ones presented in Table 7.

Table 4. Non-dimensional deflection and stress components (R = 5).

Models	$\bar{w}$	$\bar{\sigma}_x^1$	$\bar{\sigma}_x^2$	$\bar{\sigma}_x^3$	$\bar{\sigma}_y^1$	$\bar{\sigma}_y^2$	$\bar{\sigma}_y^3$	$\bar{\tau}_{xz}^1$	$\bar{\tau}_{xz}^2$
HSDT [4]	256.13	62.38	46.91	9.382	38.93	30.33	6.065	3.089	2.566
Exact [31]	258.97	60.353	46.623	9.34	38.491	30.097	6.161	4.3641	3.2675
Ferreira [32]	258.834	60.088	46.372	9.274	-	-	-	3.880	1.731
Ferreira [27]	258.180	60.0262	46.3926	9.2785	38.3644	30.0294	6.0059	4.095	2.0418
Q4, (4 × 4)	259.5352	55.923	42.7778	8.5556	36.8245	28.6415	5.7283	2.9135	1.2510
Q4, (10 × 10)	258.8336	59.5704	45.9692	9.1938	38.2179	29.8914	5.9783	3.6289	1.5831
Q4, (12 × 12)	258.8424	59.8026	46.1183	9.2237	38.3128	29.9483	5.9897	3.7122	1.6286
Q4, (20 × 20)	258.8342	60.0881	46.3718	9.2744	38.4267	30.0523	6.0105	3.8804	1.7314
Q9, (4 × 4)	258.5895	60.3915	46.942	9.3884	38.6598	30.4271	6.0854	4.0522	1.8705
Q9, (10 × 10)	258.8281	60.2736	46.556	9.3112	38.4985	30.127	6.0254	4.0669	1.9366
Q9, (12 × 12)	258.8314	60.2689	46.5404	9.3081	38.4972	30.1202	6.024	4.0719	1.952
Q9, (20 × 20)	258.8342	60.2607	46.5197	9.3039	38.4959	30.1124	6.0225	4.0841	1.9826

Table 5. Non-dimensional deflection and stress components (R = 10).

Models	$\bar{w}$	$\bar{\sigma}_x^1$	$\bar{\sigma}_x^2$	$\bar{\sigma}_x^3$	$\bar{\sigma}_y^1$	$\bar{\sigma}_y^2$	$\bar{\sigma}_y^3$	$\bar{\tau}_{xz}^1$	$\bar{\tau}_{xz}^2$
HSDT [4]	152.33	64.65	51.31	5.131	42.83	33.97	3.397	3.147	2.587
Exact [31]	159.38	65.332	48.857	4.903	43.566	33.413	3.5	4.0959	3.5154
Ferreira [32]	159.476	65.047	48.576	4.858	-	-	-	3.792	1.928
Ferreira [27]	158.9117	64.9927	48.6009	4.8601	43.4907	33.4089	3.3409	3.9803	2.3325
Q4, (4 × 4)	162.0181	60.543	44.4486	4.4449	41.9587	31.8772	3.1877	2.8323	1.3629
Q4, (10 × 10)	159.6822	64.4631	48.1314	4.8131	43.3636	33.2797	3.328	3.5483	1.747
Q4, (12 × 12)	159.6097	64.7366	48.2823	4.8282	43.4708	33.3274	3.3327	3.6295	1.8016
Q4, (20 × 20)	159.4757	65.0473	48.5758	4.8576	43.5805	33.4408	3.3441	3.7918	1.9279
Q9, (4 × 4)	159.3758	65.4971	49.2619	4.9262	43.932	33.9226	3.3923	3.8726	2.007
Q9, (10 × 10)	159.4047	65.2546	48.782	4.8782	43.6564	33.5212	3.3521	3.9533	2.1755
Q9, (12 × 12)	159.4053	65.2476	48.7654	4.8765	43.6535	33.5134	3.3513	3.9621	2.2073
Q9, (20 × 20)	159.4058	65.2373	48.7433	4.8743	43.6505	33.5042	3.3504	3.9779	2.2689

Table 6. Non-dimensional deflection and stress components (R = 15).

Models	$\bar{w}$	$\bar{\sigma}_x^1$	$\bar{\sigma}_x^2$	$\bar{\sigma}_x^3$	$\bar{\sigma}_y^1$	$\bar{\sigma}_y^2$	$\bar{\sigma}_y^3$	$\bar{\tau}_{xz}^1$	$\bar{\tau}_{xz}^2$
HSDT [4]	110.43	66.62	51.97	3.465	44.92	35.41	2.361	3.035	2.691
Exact [31]	121.72	66.787	48.299	3.238	46.424	34.955	2.494	3.9638	3.5768
Ferreira [32]	121.871	66.490	48.000	3.200	-	-	-	3.730	2.019
Ferreira [27]	121.3474	66.4362	48.0104	3.2007	46.3849	34.9650	2.331	3.9024	2.4811
Q4, (4 × 4)	125.0593	61.9463	43.5915	2.9061	44.8984	33.3497	2.2233	2.7739	1.4016
Q4, (10 × 10)	122.1499	65.8759	47.5395	3.1693	46.2623	34.8631	2.3242	3.4912	1.8158
Q4, (12 × 12)	122.0484	66.1709	47.6863	3.1791	46.3774	34.9007	2.3267	3.5712	1.8766
Q4, (20 × 20)	121.8709	66.4903	48.0001	3.2	46.4797	35.0191	2.3346	3.7297	2.0192
Q9, (4 × 4)	121.8099	67.0141	48.6933	3.2462	46.8978	35.5358	2.3691	3.7749	2.0626
Q9, (10 × 10)	121.7767	66.7069	48.2131	3.2142	46.5567	35.1012	2.3401	3.8804	2.3078
Q9, (12 × 12)	121.7766	66.6983	48.1976	3.2132	46.5525	35.0931	2.3395	3.8899	2.3516
Q9, (20 × 20)	121.7765	66.6866	48.1768	3.2118	46.5478	35.0835	2.3389	3.9054	2.433

Table 7. Non-dimensional deflection and stress components (k = 5/6).

Models	$\bar{w}$	$\bar{\sigma}_x^1$	$\bar{\sigma}_x^2$	$\bar{\sigma}_x^3$	$\bar{\sigma}_y^1$	$\bar{\sigma}_y^2$	$\bar{\sigma}_y^3$	$\bar{\tau}_{xz}^1$	$\bar{\tau}_{xz}^2$
R = 5									
Exact [31]	258.97	60.353	46.623	9.34	38.491	30.097	6.161	4.3641	3.2675
Ferreira [32]	258.834	60.088	46.372	9.274	-	-	-	3.880	1.731
Ferreira [27]	258.180	60.0262	46.3926	9.2785	38.3644	30.0294	6.0059	4.095	2.0418
Q4	258.8342	60.0881	46.3718	9.2744	38.4267	30.0523	6.0105	3.8804	1.7314
Q9	258.8342	60.2607	46.5197	9.3039	38.4959	30.1124	6.0225	4.0841	1.9826
Q4, k = 5/6	267.1507	59.9246	45.9070	9.1814	38.7909	30.2055	6.0411	3.8675	1.7430
Q9, k = 5/6	267.1177	60.0977	46.0558	9.2112	38.8587	30.2646	6.0529	4.0667	1.9980
R = 10									
Exact [31]	159.38	65.332	48.857	4.903	43.566	33.413	3.5	4.0959	3.5154
Ferreira [32]	159.476	65.047	48.576	4.858	-	-	-	3.792	1.928
Ferreira [27]	158.9117	64.9927	48.6009	4.8601	43.4907	33.4089	3.3409	3.9803	2.3325
Q4	159.4757	65.0473	48.5758	4.8576	43.5805	33.4408	3.3441	3.7918	1.9279
Q9	159.4058	65.2373	48.7433	4.8743	43.6505	33.5042	3.3504	3.9779	2.2689
Q4, k = 5/6	167.4872	64.7566	47.6721	4.7672	44.2484	33.6886	3.3689	3.7697	1.9447
Q9, k = 5/6	167.3863	64.9468	47.8409	4.7841	44.3164	33.7511	3.3751	3.9513	2.2977
R = 15									
Exact [31]	121.72	66.787	48.299	3.238	46.424	34.955	2.494	3.9638	3.5768
Ferreira [32]	121.871	66.490	48.000	3.200	-	-	-	3.730	2.019
Ferreira [27]	121.3474	66.4362	48.0104	3.2007	46.3849	34.9650	2.331	3.9024	2.4811
Q4	121.8709	66.4903	48.0001	3.2	46.4797	35.0191	2.3346	3.7297	2.0192
Q9	121.7765	66.6866	48.1768	3.2118	46.5478	35.0835	2.3389	3.9054	2.433
Q4, k=5/6	129.7105	66.1127	46.7050	3.1137	47.4140	35.3295	2.3553	3.6995	2.0400
Q9, k=5/6	129.5865	66.3085	46.8830	3.1255	47.4803	35.3936	2.3596	3.8704	2.4703

As it is possible to conclude, and as expected, the use of a shear correction equal to 5/6, produces alterations in the different quantities presented. In the present cases, the agreement with the reference solutions is better when k = 1.

3.1.2. Fundamental Frequencies of Laminated Plates with Different Stiffness Ratios

This second validation study, considers a cross-ply simply supported laminated plate with the following stacking sequence [0º/90º/90º/0º]. The thickness-to-span ratio h/a is 0.2 and the thickness of all the plies is equal. The material properties of the composite are $E_1/E_2 = 10,\ 20,\ 30,\ 40$; $G_{12} = G_{13} = 0.6E_2;\ G_{23} = 0.5E_2;\ \nu_{12} = 0.25$. Table 8 presents the fundamental frequency in a non-dimensional form using the multiplier $\bar{\omega} = \frac{\omega a^2}{h}\sqrt{\frac{\rho}{E_2}}$.

From Table 8 it is possible to conclude on the good agreement with the reference results for the different stiffness ratios considered. As we may conclude, in these cases the use of a unit shear correction factor yields a better agreement when compared to the use of a 5/6 shear correction factor.

Table 8. Non-dimensional fundamental frequency. Different stiffness ratios.

k	Method	10	20	30	40
1	Liew et al. [33]	8.2924	9.5613	10.320	10.849
	Khdeir et al. [34]	8.2982	9.5671	10.326	10.854
	Ferreira et al. [28]	8.5846	9.8384	10.5695	10.0649
1	Present (11 × 11)	8.4255	9.5735	10.2072	10.62
	Present (15 × 15)	8.4244	9.5724	10.2063	10.6192
	Present (19 × 19)	8.4241	9.5722	10.2061	10.619
5/6	Present (11 × 11)	8.14	9.1314	9.6646	10.0078
	Present (15 × 15)	8.1389	9.1305	9.6638	10.0071
	Present (19 × 19)	8.1387	9.1303	9.6636	10.0069

3.1.3. Natural Frequencies of a Composite Laminated Plate

In this second validation study, one has considered a simply supported square laminated plate with the following stacking sequence [0º/90º/90º/0º]. The side-to-thickness ratio a/h is set to 10 and the thickness of each ply is $h/3$. The material properties of the composite are: $E_1 = 173\ MPa$; $E_2 = 33.1\ MPa;\ G_{12} = 9.38\ MPa;\ G_{13} = 8.27\ MPa;\ G_{23} = 3.24\ MPa;\ \nu_{12} = 0.036;\ \nu_{13} = 0.25;$ $\nu_{23} = 0.171$. For illustrative purposes, we present in Figure 5 the corresponding first eight vibration modes.

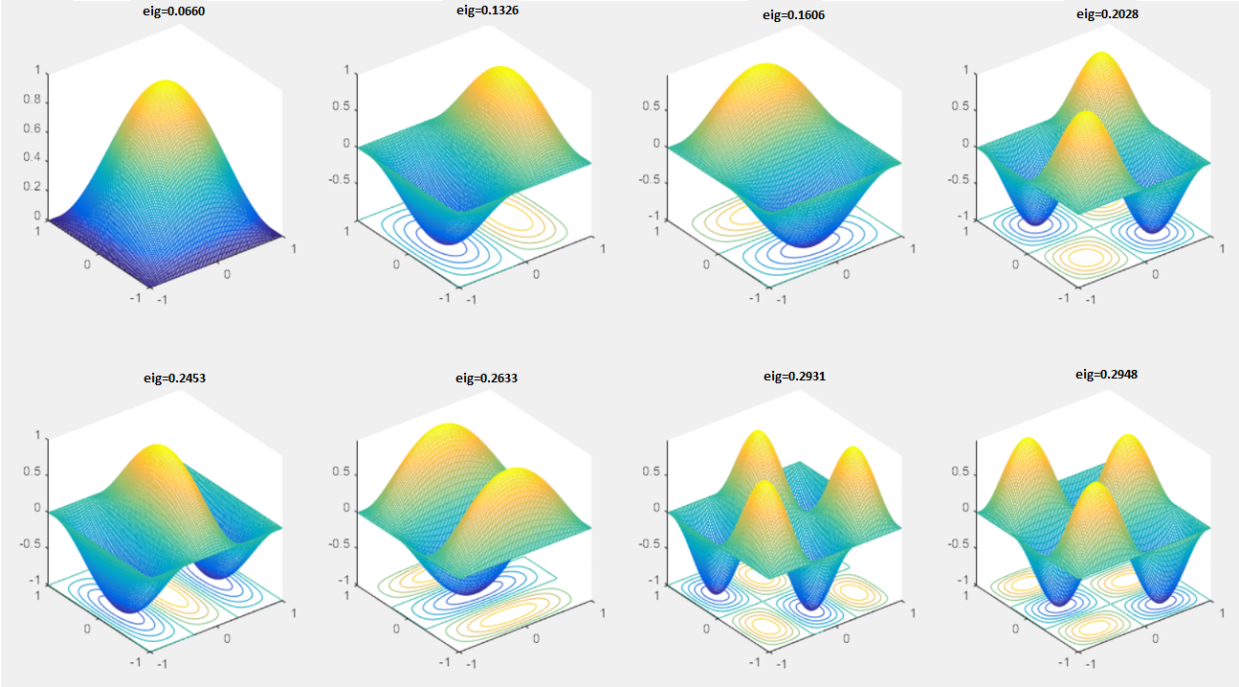

Figure 5. First eight vibration modes of the laminated plate.

The results obtained in the free vibrations analyses carried out, are presented in Table 9.

Table 9. Non-dimensional natural frequencies for the laminate plate.

Method	(1, 1)	(1, 2)	(2, 1)	(2, 2)	(1, 3)	(2, 3)	(3, 1)	(3, 2)
Exact [35]	0.0672	0.1281	0.1722	0.2080	-	-	-	-
Nosier et al. [22]	0.0672	0.1282	0.1723	0.2081	-	-	-	-
Ferreira et al. [27]	0.0681	0.1322	0.1762	0.2150	0.2376	0.2954	0.3009	0.3288
Present, (4 × 4)	0.0687	0.1277	0.1829	0.2166	0.2263	0.2882	0.3175	0.3397
Present, (10 × 10)	0.0687	0.127	0.1817	0.2155	0.2195	0.2836	0.3099	0.3286
Present, (12 × 12)	0.0687	0.1269	0.1817	0.2155	0.2194	0.2836	0.3098	0.3281
Present, (20 × 20)	0.0687	0.1269	0.1817	0.2155	0.2193	0.2835	0.3097	0.3277

The frequencies in Table 9 are non-dimensionalized using the corresponding multiplier in Eqn. 16. We can also observe a general good agreement with the reference results.

3.2. Case Studies

3.2.1. Influence of Core on the Static and Free Vibrations of a Sandwich Plate with Composite Skins

Following the previous validation studies, we considered a case study where the inner layer, the core, was made from different density polyvinyl chloride (PVC) foams [30]. This configuration is able to present a favorable lightweight solution, namely when the structure weight can be a constraint.

To this purpose one has studied the effect of considering different foams with different thicknesses. The outer layers, were assumed to be made of unidirectional carbon-epoxy or glass-epoxy composite. The material properties are presented in Tables 1 and 2, and an aspect ratio a/h = 10 was considered. The plates were subjected to a uniformly distributed transverse load (1 Pa). The maximum deflection and the first five natural frequencies for a sandwich configuration with carbon-epoxy skins and a core with 10 mm and 15 mm thickness are respectively presented in Tables 10 and 11, in a non-dimensional form. The thickness of each skin is 2 mm, in both cases.

Table 10. Non-dimensional deflection and frequencies. Carbon-epoxy skins, 10 mm core.

Core Id.	Material Id.	Deflection	Vibration modes				
			(1, 1)	(2, 1)	(1, 2)	(2, 2)	(3, 1)
1	H35	2.35E−07	0.0303	0.0489	0.0619	0.0723	0.0736
2	H45	2.16E−07	0.0316	0.0511	0.064	0.0758	0.0765
3	H60	1.72E−07	0.0354	0.0576	0.0707	0.085	0.0859
4	H80	1.45E−07	0.0385	0.0629	0.0767	0.0924	0.0944
5	H100	1.16E−07	0.0431	0.0703	0.0858	0.1034	0.1067
6	H130	9.43E−08	0.0478	0.0777	0.0959	0.1153	0.1193
7	H160	8.47E−08	0.0504	0.0817	0.1019	0.1222	0.1263
8	H200	7.41E−08	0.0539	0.0869	0.1101	0.1314	0.1354
9	H250	6.32E−08	0.0584	0.0934	0.1213	0.1438	0.1469

From Table 10, we see that as we go from the H35 to the H250 foam core, the maximum deflection decreases, which is expected as the foams provide an increasing stiffness to the plate. Concerning to the frequencies we observe an opposite trend as expected. Table 11 presents now a similar set of studies, considering a thicker core.

Table 11. Non-dimensional deflection and frequencies. Carbon-epoxy skins, 15 mm core.

Core Id.	Material Id.	Deflection	Vibration modes				
			(1, 1)	(2, 1)	(1, 2)	(2, 2)	(3, 1)
1	H35	2.64E−07	0.0285	0.0465	0.0541	0.0659	0.0688
2	H45	2.41E−07	0.0298	0.0487	0.0565	0.0689	0.0722
3	H60	1.91E−07	0.0335	0.0550	0.0639	0.0779	0.0822
4	H80	1.60E−07	0.0366	0.0600	0.0702	0.0856	0.0906
5	H100	1.27E−07	0.0411	0.0671	0.0799	0.0969	0.1024
6	H130	1.03E−07	0.0456	0.0740	0.0903	0.1089	0.1144
7	H160	9.28E−08	0.0481	0.0778	0.0965	0.1158	0.1210
8	H200	8.13E−08	0.0514	0.0826	0.1048	0.1250	0.1295
9	H250	6.94E−08	0.0557	0.0887	0.1161	0.1373	0.1403

Again we observe that the maximum deflection decreases for the higher density cores configurations, and the frequencies increase. We see additionally that in this last situation, where the

core is thicker but the skins have the same thickness, we achieve a less stiff solution, which would be expectable.

The identification of the core material in the horizontal axis of the graphics, correspond to the core identification in Tables 10 and 11, CE and GE denotes the carbon-epoxy and glass-epoxy skins.

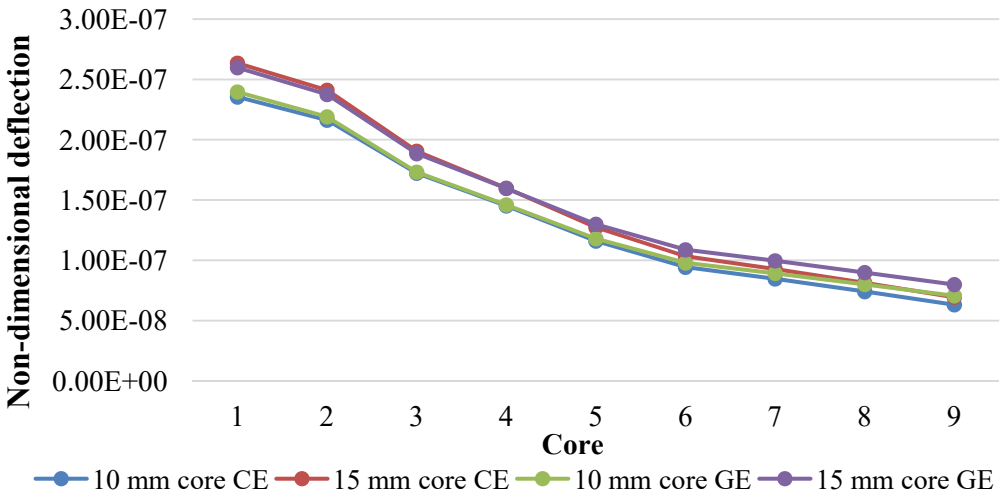

Figure 6. Non-dimensional maximum deflection of sandwich plates.

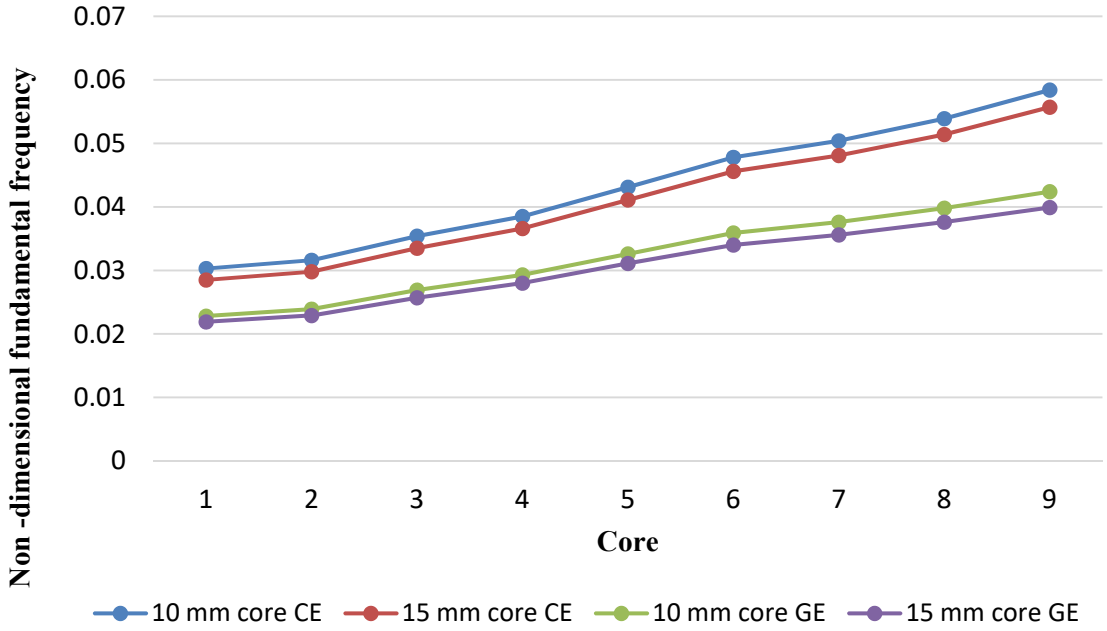

Figure 7. Non-dimensional fundamental frequency of sandwich plates.

Similar trends are observed if one considers glass-epoxy skins, as depicted in Figures 6 and 7. In addition to the stiffening effect provided by the two types of skins at different distances from the middle-plane, it is also worth of mention the evolution of the Young's modulus and the density for

the different cores configurations considered. We may conclude from the material data (Table 2) that we have a greater gradient in the case of the Young's modulus, although for the second core, the evolution rate of the Young's modulus is lower. Considering these aspects, the static and dynamic response of the sandwich plate in the neighborhood of this second configuration becomes clearer.

Also concerning to the remaining response evolution, the evolution rate of the Young's modulus slows down again in the case of the seventh core, but not the density one. This is again visible in the responses (Figures 6 and 7). Globally, we can conclude that despite the proximity perception of the curves which may be affected by the magnitude of the different scales' axes; the thicker these cores are, the greater the deflection and the minor the fundamental frequency of the sandwich plate. Moreover, when we consider a growing density core, regardless its thickness, the fundamental frequency increases and the deflection decreases.

3.2.2. Influence of Geometric Ratios on the Static and Free Vibrations of Three-Layered Composite Plate

In order to characterize the influence of plate aspect ratio (a/h) in its mechanical response, we considered a unit edge length, simply supported square laminated plate [0º/90º/0º], subjected to a uniformly distributed transverse load (1 Pa) and three side-to-thickness ratios (a/h = 5, 10 and 20). The material properties of the carbon-epoxy composite used in the plate are listed in Table 1, and the transverse displacement and the stress components are presented in non-dimensional form.

In Table 12 we can observe the non-dimensional transverse displacement and stresses for the three aspect ratios. Additionally we can also see how the plate behaves if for each a/h we consider the variation of the skins thicknesses in an equal manner. We can conclude that as the aspect ratio (a/h) increases, the plate goes thinner and the non-dimensional transverse displacement also increases.

Table 12. Non-dimensional transverse deflection and stresses vs. ratio a/h.

a/h	h_k	$\bar{w}$	$\bar{\sigma}_x^1$	$\bar{\sigma}_x^2$	$\bar{\sigma}_x^3$	$\bar{\sigma}_y^1$	$\bar{\sigma}_y^2$	$\bar{\sigma}_y^3$	$\bar{\tau}_{xz}^1$	$\bar{\tau}_{xz}^2$
5	h/6	1.48E−09	19.5679	13.0317	0.8189	1.3064	0.7513	11.3281	2.4376	1.2329
	h/5	1.50E−09	18.5382	11.2410	0.7236	1.3899	0.7205	11.1640	2.6190	1.3573
	h/4	1.57E−09	17.5487	9.1203	0.6083	1.5917	0.6740	10.7743	2.8794	1.5397
	h/3	1.72E−09	16.7142	6.2640	0.4399	1.9373	0.5558	9.1840	3.2748	1.8389
10	h/6	1.50E−08	78.2689	52.1422	3.3108	4.8995	3.1501	48.0947	4.8990	2.4775
	h/5	1.51E−08	76.6934	46.1283	2.9489	4.9249	2.8708	44.1609	5.3622	2.7893
	h/4	1.53E−08	75.1630	37.9595	2.4446	4.9481	2.4378	37.7885	5.9820	3.2284
	h/3	1.59E−08	73.8013	25.3755	1.6389	5.4659	1.6997	27.4375	6.8049	3.8884
20	h/6	2.05E−07	313.4683	208.9234	13.3188	19.4379	12.8451	196.9901	9.8338	4.9746
	h/5	2.05E−07	311.7869	187.1772	11.9098	19.1397	11.4128	174.6566	10.8530	5.6574
	h/4	2.05E−07	309.2712	155.0268	9.8104	18.4756	9.2265	141.4401	12.1659	6.5958
	h/3	2.06E−07	304.6326	102.3482	6.3685	19.2816	6.2762	102.4880	13.7655	7.9295

A similar response pattern is visible in the case of the stresses. For a specific a/h when we consider the thickening of the skins (h_k) we can conclude that the increasing trend also occurs for the transverse displacement. In the case of the evolution of stresses, it shows a similar consistent trend.

In Table 13 it is also possible to see the first four non-dimensional natural frequencies, for the same aspect ratios and skins' thicknesses.

Table 13. Non-dimensional natural frequencies vs. aspect ratio a/h.

a/h	h_k	(1, 1)	(2, 1)	(1, 2)	(2, 2)
5	h/6	0.3811	0.6345	0.8080	0.9135
	h/5	0.3774	0.6037	0.8158	0.8883
	h/4	0.3694	0.5804	0.7996	0.8661
	h/3	0.3535	0.5501	0.7645	0.8537
10	h/6	0.1216	0.2339	0.3189	0.3812
	h/5	0.1211	0.2222	0.3223	0.3631
	h/4	0.1199	0.2054	0.3228	0.3365
	h/3	0.1172	0.1828	0.3005	0.3164
20	h/6	0.0331	0.0725	0.0993	0.1216
	h/5	0.0331	0.0671	0.1024	0.1211
	h/4	0.0330	0.0600	0.1052	0.1090
	h/3	0.0328	0.0513	0.0888	0.1067

Regarding the natural frequencies, it is possible to see that as the aspect ratio increases, the natural frequencies decrease. This pattern trend is also visible when the thickness of the middle layer decreases.

3.2.3. Influence of Fiber Orientation on the Static and Free Vibrations of Three-Layered Composite Plate

To characterize the effect of the fibers' orientations on the static and free vibration behavior of the previous plates, we carried out another study. To this purpose we have considered three types of laminates, which stacking sequences may be summarized as [θº/0º/θº], [−θº/0º/θº] and [−θº/90º/θº]. The material properties of the composite and the aspect ratios considered were the same of the previous case study and the transverse displacement and the stress components are again presented in a non-dimensional form. The results obtained are presented in Tables 14 to 15.

From Table 14 it is possible to conclude that angle-ply and cross-ply three-layered laminates perform more conservatively specially for thick and moderately thick laminates. The results obtained for the stresses' components are in accordance with this.

The natural frequencies in Table 15 present a consistent trend with the Table 14 results.

When the outer plies do not follow the same unidirectional angle of the core, the fundamental frequency, as well as the other higher order frequencies, becomes higher, being higher in the case of the 45º outer plies' laminate. Again this effect is more significant for thicker plates. From these results, one may conclude that the better stacking sequence concerning the minimum transverse

deformation and the maximum fundamental frequency is presented the [45º/0º/45º] laminate. In Table 16, we can now observe the static response of the plates that possess a symmetric orientation angle in the outer layers.

Table 14. Non-dimensional deflection and stress components for the [θº/0º/θº] laminates.

a/h	*Stacking sequence*	$\bar{w}$	$\bar{\sigma}_x^1$	$\bar{\sigma}_x^2$	$\bar{\sigma}_x^3$	$\bar{\sigma}_y^1$	$\bar{\sigma}_y^2$	$\bar{\sigma}_y^3$	$\bar{\tau}_{xz}^1$	$\bar{\tau}_{xz}^2$
5	[0º/0º/0º]	2.14E−09	18.8606	2.2167	2.2167	2.5442	0.7787	0.7787	3.0414	1.9686
	[30º/0º/30º]	1.70E−09	12.0237	3.3023	4.3633	5.5495	1.3426	0.5884	2.5117	1.6649
	[45º/0º/45º]	1.53E−09	8.1046	2.3263	3.4907	8.3541	2.5853	0.5242	2.2195	1.4765
	[60º/0º/60º]	1.56E−09	5.1650	1.1668	5.3923	12.4994	3.1178	0.4897	1.9449	1.1327
	[90º/0º/90º]	1.72E−09	1.9373	0.5558	9.1840	16.7142	6.2640	0.4399	1.3839	0.6264
10	[0º/0º/0º]	1.78E−08	76.2657	20.5571	20.5571	6.5166	2.0940	2.0940	6.8372	3.9905
	[30º/0º/30º]	1.60E−08	47.4375	12.7804	27.0856	19.6930	5.5572	2.1496	5.7971	3.3289
	[45º/0º/45º]	1.50E−08	30.1627	8.2030	24.8592	30.6463	8.8301	2.3782	5.0787	2.9633
	[60º/0º/60º]	1.53E−08	19.5482	5.9614	25.8571	48.5890	15.2072	2.3090	4.5459	2.2036
	[90º/0º/90º]	1.59E−08	5.4659	1.6997	27.4375	73.8013	25.3755	1.6389	2.6868	0.9767
20	[0º/0º/0º]	2.11E−07	303.6790	96.2366	96.2366	21.9219	7.2265	7.2265	14.1760	7.8875
	[30º/0º/30º]	2.06E−07	188.8223	59.9691	129.9897	75.9990	24.3419	8.2395	12.4625	6.7458
	[45º/0º/45º]	1.98E−07	118.8191	37.7501	121.8943	119.3034	38.1318	9.3731	11.1544	6.2335
	[60º/0º/60º]	2.03E−07	76.3067	24.8855	110.2294	189.6396	62.3118	8.8632	10.8669	4.5299
	[90º/0º/90º]	2.06E−07	19.2816	6.2762	102.4880	304.6326	102.3482	6.3685	5.4941	1.7139

Table 15. Non-dimensional natural frequencies for the [θº/0º/θº] laminates.

a/h	*Stacking sequence*	(1, 1)	(2, 1)	(1, 2)	(2, 2)
5	[0º/0º/0º]	0.3184	0.5296	0.6699	0.8151
	[30º/0º/30º]	0.3568	0.5996	0.7204	0.8591
	[45º/0º/45º]	0.3759	0.6251	0.7582	0.8795
	[60º/0º/60º]	0.3727	0.6052	0.7736	0.8715
	[90º/0º/90º]	0.3535	0.5501	0.7645	0.8537
10	[0º/0º/0º]	0.1104	0.1660	0.2795	0.2838
	[30º/0º/30º]	0.1174	0.1997	0.2832	0.3055
	[45º/0º/45º]	0.1212	0.2137	0.2866	0.3167
	[60º/0º/60º]	0.1203	0.2082	0.2999	0.3166
	[90º/0º/90º]	0.1172	0.1828	0.3005	0.3164
20	[0º/0º/0º]	0.0321	0.0464	0.0768	0.1016
	[30º/0º/30º]	0.0329	0.0569	0.0900	0.0933
	[45º/0º/45º]	0.0336	0.0615	0.0900	0.0949
	[60º/0º/60º]	0.0332	0.0601	0.0949	0.0957
	[90º/0º/90º]	0.0328	0.0513	0.0888	0.1067

Table 16. Non-dimensional deflection and stress components for the [−θº/0º/θº] laminates.

a/h	*Stacking sequence*	$\bar{w}$	$\bar{\sigma}_x^1$	$\bar{\sigma}_x^2$	$\bar{\sigma}_x^3$	$\bar{\sigma}_y^1$	$\bar{\sigma}_y^2$	$\bar{\sigma}_y^3$	$\bar{\tau}_{xz}^1$	$\bar{\tau}_{xz}^2$
5	[−30º/0º/30º]	1.36E−09	10.6046	2.2560	6.1698	4.5360	0.9185	1.0381	2.2967	1.6094
	[−45º/0º/45º]	1.20E−09	7.2749	1.7780	3.3350	7.2567	1.8070	1.4519	1.9979	1.4215
	[−60º/0º/60º]	1.31E−09	4.3180	1.2189	2.7765	10.6534	3.4639	1.3589	1.6848	1.1015
10	[−30º/0º/30º]	1.18E−08	39.0379	12.3092	21.9477	15.7575	4.7019	3.4992	5.0932	3.5805
	[−45º/0º/45º]	1.05E−08	26.9461	10.9467	14.2479	27.2759	11.0915	5.0608	4.4088	3.0320
	[−60º/0º/60º]	1.17E−08	15.6310	6.4519	14.7755	40.0437	18.3180	4.6169	3.7081	2.2366
20	[−30º/0º/30º]	1.43E−07	154.4374	52.6199	80.4305	59.8252	19.7365	11.5330	10.6298	9.9229
	[−45º/0º/45º]	1.29E−07	107.6135	45.2929	59.0214	108.8538	45.8082	16.5644	9.1362	8.0365
	[−60º/0º/60º]	1.44E−07	60.4675	25.1479	61.1296	158.0092	71.2223	15.0004	7.7873	5.3613

From Table 16 we see that when the angles of the outer layers are symmetrical, the laminate presents a stiffer behavior, when compared to the configuration in Table 14. One may also conclude that the better stacking sequence concerning the minimum transverse deflection is given by the [−45º/0º/45º] configuration. In Table 17, for the same laminates, we may conclude on a similar pattern in the opposite sense (maximum frequencies values) concerning the natural frequencies.

Table 17. Non-dimensional natural frequencies for the [−θº/0º/θº] laminates.

a/h	*Stacking sequence*	(1, 1)	(2, 1)	(1, 2)	(2, 2)
5	[−30º/0º/30º]	0.3976	0.6774	0.7444	0.9865
	[−45º/0º/45º]	0.4220	0.7353	0.7778	1.0323
	[−60º/0º/60º]	0.4050	0.6630	0.8061	0.9850
10	[−30º/0º/30º]	0.1361	0.2424	0.2994	0.3875
	[−45º/0º/45º]	0.1441	0.2859	0.2915	0.4243
	[−60º/0º/60º]	0.1368	0.2458	0.3171	0.3849
20	[−30º/0º/30º]	0.0393	0.0737	0.0999	0.1216
	[−45º/0º/45º]	0.0415	0.0906	0.0914	0.1458
	[−60º/0º/60º]	0.0392	0.0757	0.1013	0.1267

Next, in Table 18, we present, the non-dimensional maximum deflection and stress components for the [−θº/90º/θº] lamination, where the lamination [−45º/90º/45º] shows to be more favorable, similarly with the results in Table 16, due to the equal thicknesses configuration considered.

A similar conclusion concerning the more favorable stacking configuration, may be drawn for the fundamental frequency and higher ones, in Table 19.

Table 18. Non-dimensional deflection and stress components for the [−θº/90º/θº] laminates.

a/h	*Stacking sequence*	$\bar{w}$	$\bar{\sigma}_x^1$	$\bar{\sigma}_x^2$	$\bar{\sigma}_x^3$	$\bar{\sigma}_y^1$	$\bar{\sigma}_y^2$	$\bar{\sigma}_y^3$	$\bar{\tau}_{xz}^1$	$\bar{\tau}_{xz}^2$
5	[0º/90º/0º]	1.72E−09	16.7142	6.2640	0.4399	1.9373	0.5558	9.1840	3.2748	1.8389
	[−30º/90º/30º]	1.31E−09	10.6534	3.4639	1.3589	4.3180	1.2189	2.7765	2.6221	1.8097
	[−45º/90º/45º]	1.20E−09	7.2567	1.8070	1.4519	7.2749	1.7780	3.3350	2.1744	1.6364
	[−60º/90º/60º]	1.36E−09	4.5360	0.9185	1.0381	10.6046	2.2560	6.1698	1.7903	1.2796
10	[0º/90º/0º]	1.59E−08	73.8013	25.3755	1.6389	5.4659	1.6997	27.4375	6.8049	3.8884
	[−30º/90º/30º]	1.17E−08	40.0437	18.3180	4.6169	15.6310	6.4519	14.7755	5.3656	4.9047
	[−45º/90º/45º]	1.05E−08	27.2759	11.0915	5.0608	26.9461	10.9467	14.2479	4.4455	4.3578
	[−60º/90º/60º]	1.18E−08	15.7575	4.7019	3.4992	39.0379	12.3092	21.9477	3.4952	2.9696
20	[0º/90º/0º]	2.06E−07	304.6326	102.3482	6.3685	19.2816	6.2762	102.4880	13.7655	7.9295
	[−30º/90º/30º]	1.44E−07	158.0092	71.2223	15.0004	60.4675	25.1479	61.1296	10.8575	14.2759
	[−45º/90º/45º]	1.29E−07	108.8538	45.8082	16.5644	107.6135	45.2929	59.0214	9.0321	12.3551
	[−60º/90º/60º]	1.43E−07	59.8252	19.7365	11.5330	154.4374	52.6199	80.4305	7.0534	7.9900

Table 19. Non-dimensional natural frequencies for the [−θº/90º/θº] laminates.

a/h	*Stacking sequence*	(1, 1)	(2, 1)	(1, 2)	(2, 2)
5	[0º/90º/0º]	0.3535	0.5501	0.7645	0.8537
	[−30º/90º/30º]	0.4050	0.6630	0.8061	0.9850
	[−45º/90º/45º]	0.4220	0.7353	0.7778	1.0323
	[−60º/90º/60º]	0.3976	0.6774	0.7444	0.9865
10	[0º/90º/0º]	0.1172	0.1828	0.3005	0.3164
	[−30º/90º/30º]	0.1368	0.2458	0.3171	0.3849
	[−45º/90º/45º]	0.1441	0.2859	0.2915	0.4243
	[−60º/90º/60º]	0.1361	0.2424	0.2994	0.3875
20	[0º/90º/0º]	0.0328	0.0513	0.0888	0.1067
	[−30º/90º/30º]	0.0392	0.0757	0.1013	0.1267
	[−45º/90º/45º]	0.0415	0.0906	0.0914	0.1458
	[−60º/90º/60º]	0.0393	0.0737	0.0999	0.1216

In Figure 8, by comparing the three sets of the previous deflection results for an aspect ratio a/h = 10, we conclude that for the studied laminations, the solution [−45º/0º/45º] provide a stiffer plate.

Similarly for the non-dimensional fundamental frequency, presented in Figure 9, we arrive at a similar conclusion, concerning the maximization of that frequency.

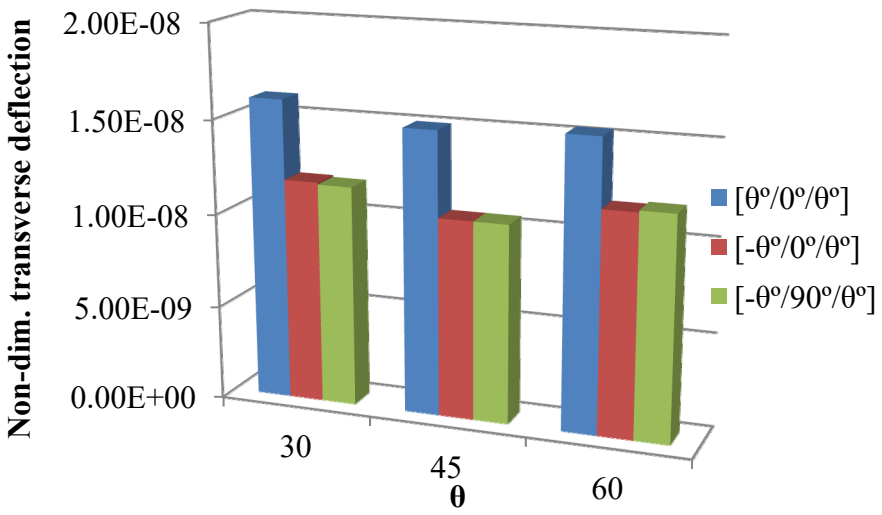

Figure 8. Non-dimensional transverse deflections. Different laminations.

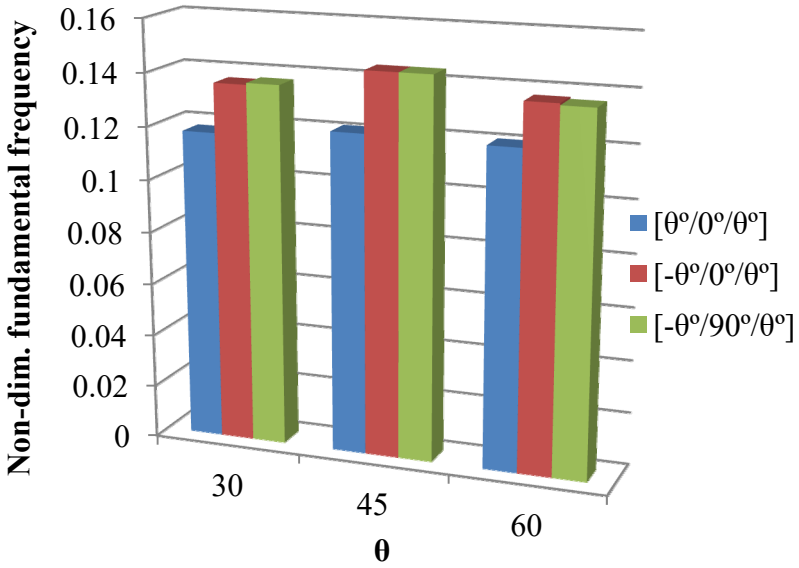

Figure 9. Non-dimensional fundamental frequencies. Different laminations.

From the different configurations considered, it is possible to conclude that stacking sequences [−45º/90º/45º] and [−45º/0º/45º] would perform better.

3.2.4. Influence of Fiber Material on the Static and Free Vibrations of Three-Layered Composite Plate

In this case study, one intends to assess the static and free vibration behavior of three-layered plates, having the same matrix phase and different reinforcement fibers. To the purpose of this study we have considered a fixed stacking sequence, namely [30º/0º/30º] maintaining the same equal

thickness in all layers. The boundary conditions, loading and the discretization used are identical to the ones in the previous case studies. The material properties used in the present case, are shown in Table 1. Again the results are presented in a non-dimensional form. The results obtained can be observed in Table 20 and in Figure 10 and 11, respectively for the static and free vibrations analyses. In Table 20, GE and CE represent respectively the glass-epoxy and the carbon-epoxy composite.

Table 20. Non-dimensional deflection and stress components.

Vf = 0.6	*a/h*	$\bar{w}$	$\bar{\sigma}_x^1$	$\bar{\sigma}_x^2$	$\bar{\sigma}_x^3$	$\bar{\sigma}_y^1$	$\bar{\sigma}_y^2$	$\bar{\sigma}_y^3$	$\bar{\tau}_{xz}^1$	$\bar{\tau}_{xz}^2$
GE	5	2.01E−09	8.8353	2.0988	2.7273	6.0754	1.6864	1.3079	2.3512	1.4542
	10	2.33E−08	35.5669	11.0048	14.5513	22.3650	7.1129	5.0361	5.0489	2.9002
	20	3.36E−07	142.3576	46.6049	61.7848	87.3974	28.7909	19.9212	10.4751	5.8138
CE	5	1.70E−09	12.0237	3.3023	4.3633	5.5495	1.3426	0.5884	2.5117	1.6649
	10	1.60E−08	47.4375	12.7804	27.0856	19.6930	5.5572	2.1496	5.7971	3.3289
	20	2.06E−07	188.8223	59.9691	129.9897	75.9990	24.3419	8.2395	12.4625	6.7458

From Table 20 we conclude that, as expected the carbon-epoxy composite provides a stiffer plate when compared to the glass-epoxy composite laminated plate. As previously, as the aspect ratio increases, the deflection follows the same increasing trend. The stress components accompany an identical behavior to that one already observed.

Concerning to Figure 10, it is important to note that the results are presented in a non-dimensional form (Eqn. 16). So, assuming that the linear elastic operating conditions of the structure would be not compromised, if we considered further increases in the aspect ratio, this doesn't means that the frequencies would be the same, irrespective to the material nature. As expected, also in Figure 11 we may conclude on the stiffening effect of the carbon in the composite, yielding higher fundamental frequencies regardless the aspect ratio value.

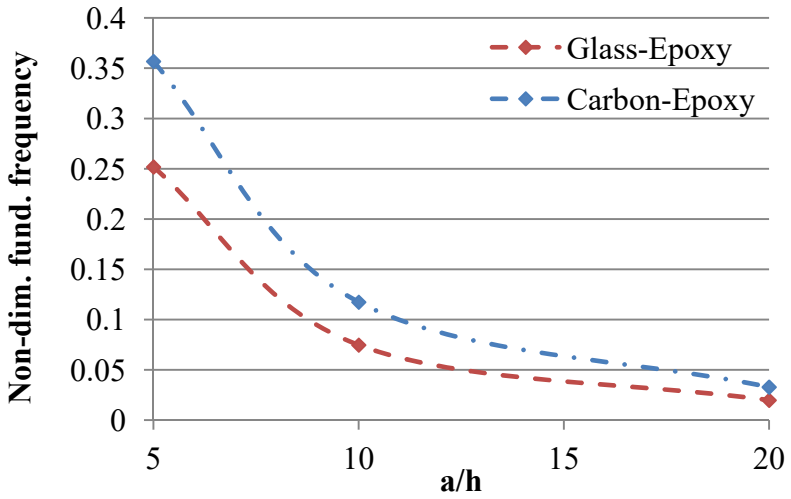

Figure 10. Non-dimensional fundamental frequency (Vf = 60%).

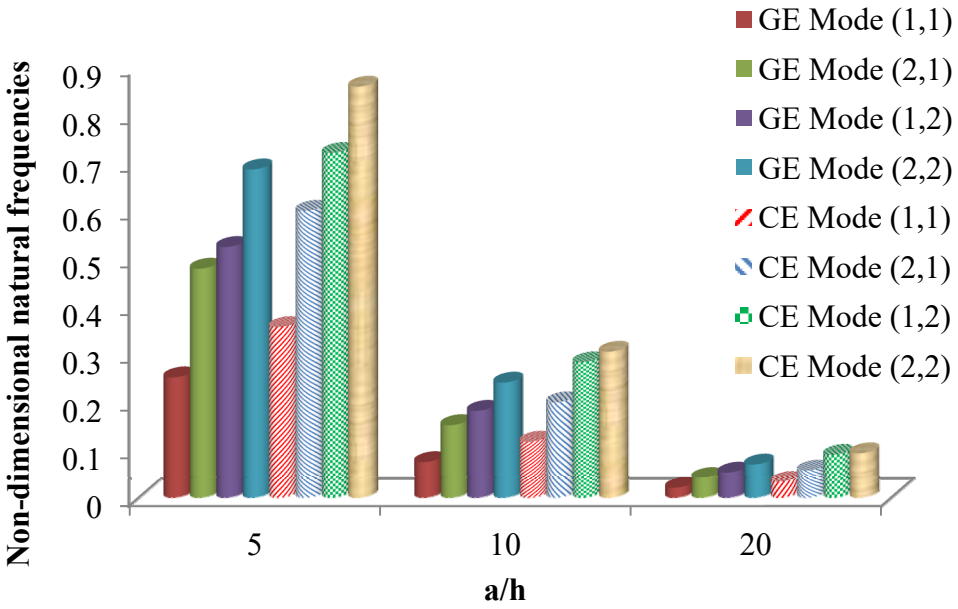

Figure 11. Non-dimensional natural frequencies. Glass-epoxy composite.

In the legend of Figure 11, GE and CE stand respectively for glass-epoxy and carbon-epoxy. From this figure we may see extended to the higher vibration modes, the conclusion that the carbon-epoxy plates present higher frequencies' values when compared to the glass-epoxy ones. It is also possible to globally observe that the natural frequencies present a decreasing trend for higher aspect ratios.

4. Conclusions

This work presents a study on the static and free vibrations response of sandwich and laminated composite plates, carried out through a first order shear deformation layerwise theory. The parametric analyses carried out allowed characterizing the influence of material and geometrical properties of these plates. Summarizing the results obtained in the different parametric studies carried out, it is possible to conclude on the importance of the sandwich core stiffness as well as on the nature of the reinforcement fiber and on the stacking sequence in the case of the three-layered fiber reinforced composite. The influence of the geometrical parameters considered namely the plate's aspect ratio and the layers thicknesses was also verified in both cases. Globally, one considers that the results obtained in this parametric study, contributes to the understanding of the static and free vibrations behavior of sandwich and three-layered composite plates. It is also relevant to add that this layerwise theory, besides the achievement of a detailed kinematics description, may be computationally less expensive when compared to other equivalent single-layer higher order theories.

Acknowledgments

The authors acknowledge the support of FCT/MEC through the Project LAETA UID/EMS/50022/2013.

Conflict of Interest

All authors declare no conflict of interest.

References

1. Reissner E (1972) A Consistent Treatment of Transverse Shear Deformations in Laminated Anisotropic Plates. *AIAA J* 10: 716–718.
2. Whitney JM (1969) The Effect of Transverse Shear Deformation on the Bending of Laminated Plates. *J Compos Mater* 3: 534–547.
3. Lo KH, Christensen RM, Wu EM (1977) A High-Order Theory of Plate Deformation—Part 2: Laminated Plates. *J Appl Mech* 44: 669–676.
4. Pandya BN, Kant T (1988) Higher-order shear deformable theories for flexure of sandwich plates —Finite element evaluations. *Int J Solids Struct* 24: 1267–1286.
5. Bernardo GMS, Damásio FR, Silva TAN, et al. (2016) A Study on the Structural Behaviour of FGM Plates: Static and Free Vibrations Analyses. *Compos Struct* 136: 124–138.
6. Loja MAR, Barbosa JI, Soares CMM (2015) Analysis of Sandwich Beam Structures Using Kriging Based Higher Order Models. *Compos Struct* 119: 99–106.
7. Viola E, Tornabene F, Fantuzzi N (2013) General higher-order shear deformation theories for the free vibration analysis of completely doubly-curved laminated shells and panels. *Compos Struct* 95: 639–666.
8. Reddy JN (1984) A refined nonlinear theory of plates with transverse shear deformation. *Int J Solids Struct* 20: 881–896.
9. Ferreira AJM, Barbosa JT (2000) Buckling behaviour of composite shells. *Compos Struct* 50: 93–98.
10. Dehkordi MB, Khalili SMR, Carrera E (2016) Non-linear transient dynamic analysis of sandwich plate with composite face-sheets embedded with shape memory alloy wires and flexible core-based on the mixed LW (layer-wise)/ESL (equivalent single layer) models. *Compos Part B-Eng* 87: 59–74.
11. Thai HC, Nguyen-Xuan H, Bordas S, et al. (2015) Isogeometric analysis of laminated composite plates using the higher-order shear deformation theory. *Mech Adv Mater Struct* 22: 451–469.
12. Thai CH, Ferreira AJM, Bordas S, et al. (2014) Isogeometric analysis of laminated composite and sandwich plates using a new inverse trigonometric shear deformation theory. *Eur J Mech A-Solid* 43: 89–108.
13. Thai CH, Nguyen-Xuan H, Nguyen-Thanh N, et al. (2012) Static, free vibration and buckling analysis of laminated composite Reissner-Mindlin plates using NURBS-based isogeometric approach. *Int J Numer Meth Eng* 91: 571–603.
14. Thai-Hoang C, Nguyen-Thanh N, Nguyen-Xuan H, et al. (2011) An alternative alpha finite element method with discrete shear gap technique for analysis of laminated composite plates.

Appl Math Comput 217: 7324–7348.
15. Thai CH, Ferreira AJM, Carrera E, et al. (2013) Isogeometric analysis of laminated composite and sandwich plates using a layerwise deformation theory. *Compos Struct* 10: 196–214.
16. Carrera E (2003) Historical review of Zig-Zag theories for multilayered plates and shells. *Appl Mech Rev* 56: 287–308.
17. Carrera E (2003) Theories and Finite Elements for Multilayered Plates and Shells: A Unified compact formulation with numerical assessment and benchmarking. *Arch Comput Method E* 10: 215–296.
18. Demasi L, Yu W (2013) Assess the Accuracy of the Variational Asymptotic Plate and Shell Analysis (VAPAS) Using the Generalized Unified Formulation (GUF). *Mech Adv Mater Struct* 20: 227–241.
19. Filippi M, Carrera E (2016) Bending and vibrations analyses of laminated beams by using a zig-zag-layer-wise theory. *Compos Part B-Eng* 98: 269–280.
20. Ferreira AJM (2005) Analysis of Composite Plates Using a Layerwise Theory and Multiquadrics Discretization. *Mech Adv Mater Struct* 12: 99–112.
21. Vuksanović D, Ćetković M (2005) Analytical solution for multilayer plates using general layerwise plate theory. *Facta Universitatis Series: Arch Civil Eng* 3: 121–136.
22. Nosier A, Kapania RK, Reddy JN (1993) Free vibration analysis of laminated plates using a layerwise theory. *AIAA J* 31: 2335–2346.
23. Sainsbury MG, Zhang QJ (1999) The Galerkin element method applied to the vibration of damped sandwich beams. *Comput Struct* 71: 239–256.
24. Daya EM, Potier-Ferry M (2001) A numerical method for nonlinear eigenvalue problems application to vibrations of viscoelastic structures. *Comput Struct* 79: 533–541.
25. Barkanov E, Skukis E, Petitjean B (2009) Characterisation of viscoelastic layers in sandwich panels via an inverse technique. *J Sound Vib* 327: 402–412.
26. Araújo AL, Soares CMM, Soares CAM, et al. (2010) Optimal design and parameter estimation of frequency dependent viscoelastic laminated sandwich composite plates. *Compos Struct* 92: 2321–2327.
27. Ferreira AJM, Fasshauer GE, Batra RC, et al. (2008) Static deformations and vibration analysis of composite and sandwich plates using a layerwise theory and RBF-PS discretizations with optimal shape parameter. *Compos Struct* 86: 328–343.
28. Ferreira AJM, Viola E, Tornabene F, et al. (2013) Analysis of sandwich plates by generalized differential quadrature method. *Math Probl Eng* 964367: 12.
29. Reddy JN (1997) *Mechanics of laminated composite plates*. Boca Raton, Florida, USA: CRC Press.
30. DivinycellH Technical Data. Diab International AB, 252 21 Helsingborg, Sweden 2016. Available from: http://www.diabgroup.com/en-GB/Products-and-services#.
31. Srinivas S (1973) A refined analysis of composite laminates. *J Sound Vib* 30: 495–507.
32. Ferreira AJM (2010) *Problemas de Elementos Finitos*. Lisboa, Portugal: Fundação Calouste Gulbenkian.
33. Liew KM, Huang YQ, Reddy JN (2003) Vibration analysis of symmetrically laminated plates based on FSDT using the moving least squares differential quadrature method. *Comput Method Appl M* 192: 2203–2222.
34. Khdeir AA, Librescu L (1988) Analysis of symmetric cross-ply laminated elastic plates using a

higher-order theory: part II—Buckling and free vibration. *Compos Struct* 9: 259–277.
35. Srinivas S, Rao CVJ, Rao AK (1970) An exact analysis for vibration of simply-supported homogeneous and laminated thick rectangular plates. *J Sound Vib* 12: 187–199.

AIMS Press